

## REVIEW

View Article Online  
View Journal | View IssueCite this: *Mater. Chem. Front.*,  
2024, 8, 1334Received 29th October 2023,  
Accepted 14th December 2023

DOI: 10.1039/d3qm01158e

rsc.li/frontiers-materials

# A review on the photochemical synthesis of atomically dispersed catalysts

Shaohua Chen and Pengxin Liu \*

A better world calls for better catalysts. With the increasing demand for low carbon emission processes, both the efficiency and environmentally benign synthesis of catalytic materials should be considered. As an emerging synthetic method for atomically dispersed catalysts, photochemical synthesis has several advantages, including its green process and ability to precisely control the structure of active sites. This review presents the research progress over the last decade, from the very first examples to developed cases on the topic and the aspects of the synthetic strategy, mechanism analysis, and application potential. The key factors affecting the preparation of atomically dispersed catalysts by the photochemical method are thoroughly discussed. More importantly, major challenges in developing the photochemical method, among other methods for synthesizing atomically dispersed catalysts, are highlighted; suggestions are also provided. By keeping abreast of these advances, we foresee the fast and broad development of photochemical methods in the catalysis community.

## 1. Introduction

Heterogeneous supported catalysts are widely used in the chemical industry owing to their robustness and easy separation, yet their activities and utilization efficiencies of metal atoms are often significantly lower than those of homogeneous molecular catalysts.<sup>1–3</sup> To achieve better catalytic performance and higher utilization efficiency of active components, tuning the particle sizes of supported species is a well-documented strategy.

Reducing the sizes of supported active components often leads to a boost in catalyst activity, which was first demonstrated in gold-based systems; gold exhibited a high catalytic activity in catalytic CO oxidation when the sizes of the supported gold were reduced to the nanoscale.<sup>4</sup> The effect was later confirmed in other systems and was collectively termed as the “size effect”.<sup>5,6</sup> One might naturally be curious about the extreme effects in down-sizing the supported metal species and its impact on the catalytic performance, but the synthetic methods and characterization techniques in use at that time held back such a curiosity.

The concept of single-atom catalysis was proposed for the first time in 2011,<sup>7</sup> with the successful synthesis (co-

School of Physical Science and Technology, ShanghaiTech University, Shanghai  
201210, P. R. China. E-mail: liupx@shanghaitech.edu.cn



Shaohua Chen

Dr Shaohua Chen obtained his Master's degree from Nankai University and subsequently completed his PhD following his graduation in 2020, he pursued a two-and-a-half-year postdoctoral fellowship in the research group of his supervisor, Tiehong Chen. Currently, he is engaged in postdoctoral research at ShanghaiTech University under the supervision of Prof. Pengxin Liu. His research interests lie in the development and application of porous materials and atomically dispersed catalysts.



Pengxin Liu

Dr Pengxin Liu is currently an Assistant Professor at ShanghaiTech University, which he joined in 2021, after his stay at Xiamen and Zürich. He worked with Prof. Nanfeng Zheng (Xiamen Univ.) from 2010 to 2018 for his PhD and post-doctoral training and then with Prof. Christophe Copéret (ETH) from 2018 to 2021 as a Research Assistant. Inspired and influenced by his mentors, Liu is interested in the surface chemistry of nanomaterials, especially of atomically dispersed catalysts, ultrathin-structured oxides, and other model systems. He is also a public science influencer with 1 million followers.



precipitation strategy) and characterization of a Pt<sub>1</sub>/FeO<sub>x</sub> catalyst, aided by combined X-ray absorption spectroscopy (XAS), aberration-corrected scanning transmission electron microscopy (AC-STEM), and Fourier-transform infrared (FT-IR) spectroscopy. After over a decade of development, single-atom catalysis has become a central aspect of heterogeneous catalysis and has shown immense potential in areas such as energy,<sup>8–10</sup> environment,<sup>11,12</sup> and chemical synthesis.<sup>13–15</sup> It is now generally accepted that single-atom catalysts have a high atomic utilization efficiency and, therefore, a better catalytic performance in comparison to nanocatalysts.

It should be noted that the use of the term “single-atom catalyst” is not widely accepted in the field. Other terms like “atomically dispersed catalyst”,<sup>16,17</sup> and “single-atom site catalyst”,<sup>18</sup> are also in use, with “single-site catalyst” representing another class of catalysts.<sup>19–21</sup> “Single-atom catalyst” emphasizes the nuclearity, whereby the active sites of a single-atom catalyst should be mononuclear atoms/ions, but the uniformity of the structures of supported single atoms, especially the coordination structure, does not need to be uniform.<sup>2,21–25</sup> Lately, “dual-metal-sites catalyst” was also proposed to describe two different metal species in close proximity, emphasizing the nuclearity but not the uniformity of the structures.<sup>26</sup> Alternatively, “single-site catalyst” emphasizes the uniformity of active sites in the pursuit of maintaining the structural uniformity of molecular catalysts (used as precursors for the synthesis of single-site catalysts). We prefer the term “atomically dispersed catalysts” as it includes the information about the atomic dispersion and supported structure. This term is also more general, covering all kinds of “single-atom catalysts” and a part of the “single-site catalysts”.<sup>21</sup> In this work, we use the term “atomically dispersed catalysts” to describe the object of the present study.

The synthesis of spatially separated and structurally secured atomically dispersed catalysts is of great interest in both industrial catalysis and scientific research.<sup>18,27–32</sup> Significant efforts have been devoted towards achieving this goal. From different viewpoints, the synthesis of atomically dispersed catalysts can be classified into several categories: top-down methods *vs.* bottom-up methods, or conventional methods *vs.* emerging methods.<sup>29–32</sup> Some examples of bottom-up methods include the wet impregnation method, chemical vapour deposition (CVD), electrochemical method (EM), and atomic layer deposition (ALD), of which the wet impregnation method is also a conventional method to prepare traditional supported catalysts. The advantages and disadvantages of the above-mentioned methods for synthesizing atomically dispersed catalysts have been nicely summarized and reviewed.<sup>33–35</sup> Nevertheless, one emerging approach that has attracted some research interests in recent years but that still lacks a progress review is the photochemical method.

Consequently, in this review, we provide such a review, starting from the basic principles of the photochemical method, and then summarizing the research progresses on atomically dispersed catalysts prepared by this method in recent years. The preparation methods are next classified according to the different preparation conditions. Then, the

photochemical method for synthesizing atomically dispersed catalysts is compared with the method for synthesizing nanoparticles, focusing on the key factors affecting the synthesis, including the supports, ligands, sacrificial agents, light source, and temperature. Finally, based on recent developments in related fields, the key challenges and opportunities for this method are outlined, and the future development direction is also suggested.

## 2. Fundamental principles

### 2.1. Principle behind the photodeposition of nanoparticles

The photochemical method for preparing atomically dispersed catalysts was inspired by the photodeposition of nanoparticles over semiconductors, which is a well-established method to modify photocatalysts to achieve better photocatalytic performance.<sup>36</sup> Such a method dates back to 1978, when Kraeutler *et al.* accomplished the successful loading of well-dispersed Pt nanoparticles onto a TiO<sub>2</sub> support, initiating research on the optical deposition of metal (oxide) nanoparticles on semiconductor surfaces.<sup>37</sup> After decades of development, photodeposition has also been found to be useful for preparing supported catalysts for other reactions apart from just photocatalysis, as has been reviewed lately.<sup>38–40</sup> Due to its mild, simple, green, and safe reaction conditions, photodeposition methods can enable the simple, rapid, and scalable production of metal nanoparticles without deploying dangerous reagents or complex equipment, thereby exhibiting high potential for application purposes.

In general, photochemical methods employ light to stimulate chemical reactions and regulate the synthesis of nanomaterials. It is commonly accepted that the reaction process in this method typically involves three steps (Fig. 1a): (i) photoelectric separation occurs after the semiconductor absorbs photons, whereby electrons enter the conduction band (CB) from the valence band (VB), leaving holes in the VB; (ii) photogenerated electrons and holes transfer to the surface, during which some CB electrons and VB holes in the excited state may recombine and dissipate energy in the form of heat; (iii) the residual electrons or holes on the semiconductor surface chemically react with metal ions to

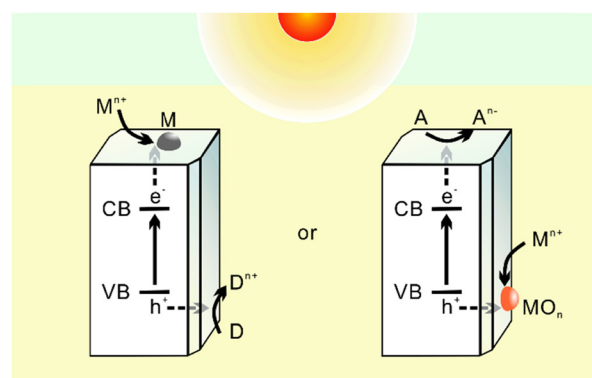
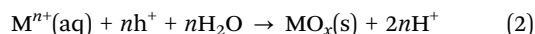
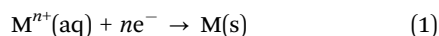


Fig. 1 Schematic diagram of reductive or oxidative photodeposition. VB: valence band, CB: conduction band, M: metal, D: electron donor, A: electron acceptor, and *n*: number of electrons (or holes) involved.



deposit them, through reductive or oxidative photodeposition. Here, reductive photodeposition (1) is initiated through the reduction of the metal precursor from  $n^+$ -valence  $M^{n+}$  to zero-valence  $M^0$  by excited electrons on the semiconductor surface, forming nuclear centres that grow and subsequently aggregate to form metal nanoparticles; while oxidative photodeposition (2) refers to the deposition of metal in the form of oxides on the semiconductor by utilizing the available holes:



Note, these equations are over-simplified and purely theoretical; whereas the true processes are much more complicated, please refer to Part 4.1.

From a mechanism understanding, one can easily conclude the principles of photodeposition: (i) the metal (oxide) being deposited must have a reduction/oxidation potential that is favourable in relation to the semiconductor band position, which means that CB should be more negative than the reduction potential of the metal, and the VB should be more positive than the oxidation potential of the oxidized substance; (ii) the photon energy of the incident light must surpass the band gap energy of the semiconductor; And (iii) the effective separation and migration of photogenerated carriers are necessary.

## 2.2. Photodeposition of single atoms

Apparently, photodeposition belongs to the category of bottom-up synthetic methods for supported catalysts. For any bottom-up method, decreasing the batching of the metal precursor to an extreme will undoubtedly lead to the formation of atomically dispersed catalysts, if the supported species can be stabilized on the surface of the chosen supports.<sup>27</sup> This is the strategy used in the first examples of preparing atomically dispersed catalysts through traditional photodeposition methods. In this regard, the loading amount of active sites would be quite low, the same as with the cases for atomically dispersed catalysts prepared through wet chemistry (impregnation, co-precipitation) or other depositions (CVD, ALD). Several improved methods have been developed since to increase the loading of active atoms, see Part 3 below.

In comparison to other bottom-up methods, the photochemical method possesses several advantages: (i) the photodeposition is a surface reaction and no other reductant/oxidant is needed; hence the photodeposition would only happen on the surface of the supports, and no phase separation (as might happen in conventional methods) would occur; (ii) the method typically requires mild reaction conditions, simple operations with a simple equipment (usually only one light source lamp), and minimal energy consumption; (iii) precise regulation of the properties of an atomically dispersed catalyst can be achieved by adjusting the light intensity, illumination time, temperature, reactant concentration, and supports. This regulation allows for customized catalytic performance through manipulation of the type, concentration, and distribution of the active sites. The method is therefore comparably more flexible. Overall, the photochemical method possesses notable advantages in comparison to conventional methods.

## 3. Photochemical synthesis of atomically dispersed catalysts

Since the photochemical method debuted, it has become a highlight in the field of single-atom catalysis. Even long before the term “single-atom catalysis” was proposed, numerous studies have shown that even atomically dispersed species could be catalytically active.<sup>41</sup> Yet, whether single atoms were truly responsible for most supported catalysts, other than the supported nanoparticles, was a long-standing debate. It was not until Maria *et al.* demonstrated that only isolated  $Au-(OH)_x$  species (photochemically produced) were active for water-gas shift reactions, while Au nanoparticles were inactive, that the question was finally answered.<sup>42</sup> We believe Maria’s work began the application of the photochemical synthetic method in the field of single-atom catalysis. Other significant milestones in the past decade are illustrated in Fig. 2. We summarize these reports into two groups, depending on the reaction conditions: liquid-phase and solid-phase photochemical syntheses.

### 3.1. Liquid-phase photochemical synthesis

The conventional photodeposition of nanoparticles typically occurs in a liquid medium, which offers a free environment for the precursors’ movement and facilitates a more uniform dispersion of supported nanoparticles in terms of their particle size and distribution. The first examples of the photochemical synthesis of atomically dispersed catalysts were also carried out in the liquid phase. The successful preparation was achieved through a selective etching, metal loading lowering, or using supports with a large surface area. Some atomically dispersed catalysts prepared by photochemical methods in the liquid phase are summarized in Table 1.

In 2013, Maria *et al.* used a combination of UV radiation and cyanide leaching to prepare a  $Au/TiO_2$  catalyst, which was the first time observable atomically dispersed  $Au-(OH)_x$  species were prepared using a photochemical method,<sup>42</sup> as depicted in Fig. 3a. They found that the cyanide leaching treatment only removed the Au nanoparticles and did not change the catalytic performance. Therefore, they drew the conclusion that in the

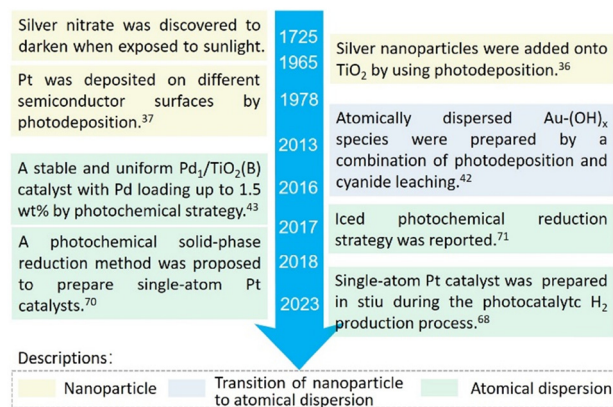


Fig. 2 Timeline of the noteworthy milestones in the preparation of atomically dispersed catalysts by the photochemical method.



**Table 1** Summarized experimental conditions for the liquid-phase photochemical syntheses of reported atomically dispersed catalysts

| Metal/support                                                     | Precursor                            | Ligand                                           | Reagent        | Light source                     | Exposure | Content      | Valence state                      | Ref. |
|-------------------------------------------------------------------|--------------------------------------|--------------------------------------------------|----------------|----------------------------------|----------|--------------|------------------------------------|------|
| Au/TiO <sub>2</sub>                                               | HAuCl <sub>4</sub>                   | —                                                | Ethanol        | 365 nm/10 mW cm <sup>-2</sup>    | 10 min   | 1.16 wt%     | Au <sup>0</sup>                    | 42   |
| Pd <sub>1</sub> /TiO <sub>2</sub> (B)                             | H <sub>2</sub> PdCl <sub>4</sub>     | EG                                               | —              | 365 nm/1.94 mW cm <sup>-2</sup>  | 10 min   | 1.5 wt%      | Pd <sup>2+</sup>                   | 43   |
| Pd/TiO <sub>2</sub> or P25                                        | H <sub>2</sub> PdCl <sub>4</sub>     | —                                                | —              | 365 nm/1.94 mW cm <sup>-2</sup>  | 10 min   | 0.1 wt%      | Pd <sup>2+</sup>                   | 44   |
| Pd/TiO <sub>2</sub> (B)                                           | H <sub>2</sub> PdCl <sub>4</sub>     | EG                                               | —              | 365 nm/1.94 mW cm <sup>-2</sup>  | 10 min   | 1.0 wt%      | Pd <sup>2+</sup>                   | 45   |
| Pd <sub>1</sub> /TiO <sub>2</sub> (anatase)                       | H <sub>2</sub> PdCl <sub>4</sub>     | CH <sub>3</sub> CN                               | —              | UV                               | 1 h      | 0.4 wt%      | Pd <sup>δ+</sup> (0 < δ < 2)       | 46   |
| Pd <sub>1</sub> /TiO <sub>2</sub> (B)                             | H <sub>2</sub> PdCl <sub>4</sub>     | EG                                               | —              | 365 nm UV/10 mW cm <sup>-2</sup> | 5 min    | 0.14 at%     | Pd <sup>δ+</sup> (0 < δ < 2)       | 47   |
| Pd/(GO/TiO <sub>2</sub> )                                         | K <sub>2</sub> PdCl <sub>6</sub>     | —                                                | —              | UV                               | 12 h     | 2 wt%        | Pd <sup>0</sup> + Pd <sup>2+</sup> | 48   |
| Pd/CeO <sub>2</sub>                                               | H <sub>2</sub> PdCl <sub>4</sub>     | —                                                | —              | 220–770 nm                       | —        | 0.88 wt%     | Pd <sup>0</sup> + Pd <sup>2+</sup> | 49   |
| Pd–EG–BiOBr                                                       | H <sub>2</sub> PdCl <sub>4</sub>     | EG                                               | —              | UV                               | 15 min   | 0.2 wt%      | Pd <sup>2+</sup>                   | 50   |
| Pd <sub>SA+NP</sub> /SAPO-31                                      | NaPdCl <sub>4</sub>                  | —                                                | Ethanol        | 365 nm/1.92 mW cm <sup>-2</sup>  | 1 h      | 0.38 wt%     | Pd <sup>0</sup> + Pd <sup>2+</sup> | 51   |
| Pd–Cds/SiO <sub>2</sub>                                           | PdCl <sub>2</sub>                    | —                                                | Ethanol        | λ > 300 nm                       | 30 min   | 1.5 wt%      | Pd <sup>2+</sup>                   | 52   |
| Pt <sub>1</sub> /TiO <sub>2</sub>                                 | H <sub>2</sub> PtCl <sub>6</sub>     | EG                                               | —              | 365 nm                           | 30 min   | 0.77 wt%     | Pt <sup>0</sup>                    | 53   |
| Pt/TiO <sub>2</sub> -A                                            | H <sub>2</sub> PtCl <sub>6</sub>     | —                                                | —              | 235 nm                           | 15 min   | 0.6 wt%      | Pt <sup>δ+</sup> (0 < δ < 2)       | 54   |
| Pt/ZnIn <sub>2</sub> S <sub>4</sub>                               | H <sub>2</sub> PtCl <sub>6</sub>     | N(C <sub>2</sub> H <sub>5</sub> OH) <sub>3</sub> | —              | > 420 nm                         | 60 min   | 0.26 wt%     | Pt <sup>δ+</sup> (2 < δ < 4)       | 55   |
| Pt/RuCeO <sub>x</sub>                                             | H <sub>2</sub> PtCl <sub>6</sub>     | —                                                | —              | 50 W UV                          | 3 h      | 0.49 wt%     | Pt <sup>2+</sup>                   | 56   |
| Pt-PVP/TNR@GC                                                     | H <sub>2</sub> PtCl <sub>6</sub>     | PVP                                              | Ethanol        | 365 nm/4.8 mW cm <sup>-2</sup>   | 30 min   | 1.75 wt%     | Pt <sup>δ+</sup> (0 < δ < 4)       | 57   |
| Pt/MCN                                                            | H <sub>2</sub> PtCl <sub>6</sub>     | —                                                | —              | UV                               | 1 h      | 3% (nominal) | Pt <sup>δ+</sup>                   | 58   |
| CoSe <sub>2-x</sub> -Pt                                           | H <sub>2</sub> PtCl <sub>6</sub>     | —                                                | —              | UV                               | 10 min   | 2.25 wt%     | Pt <sup>2+</sup>                   | 59   |
| PA-Ni@PCN/Pt-SAC                                                  | H <sub>2</sub> PtCl <sub>6</sub>     | Phytate                                          | —              | > 800 nm                         | 5 h      | 0.22 wt%     | Pt <sup>δ+</sup> + Pd <sup>0</sup> | 60   |
| Ca <sub>2</sub> Nb <sub>3</sub> O <sub>10</sub> -Pt <sub>SA</sub> | H <sub>2</sub> PtCl <sub>6</sub>     | TBA+                                             | —              | Sunlight                         | 5 min    | 0.5 wt%      | Pt <sup>2+</sup>                   | 61   |
| Ru–N/BC                                                           | RuCl <sub>3</sub>                    | Urea                                             | —              | UV                               | 2 h      | 0.41 wt%     | Pt <sup>δ+</sup> (3 < δ < 4)       | 62   |
| AgSA-SCN                                                          | AgNO <sub>3</sub>                    | Hydramines                                       | —              | UV                               | 30 min   | 1.41 wt%     | Ag <sup>δ+</sup> (0 < δ < 1)       | 63   |
| Ir–MoSe <sub>2</sub> @NiCo <sub>2</sub> Se <sub>4</sub>           | IrCl <sub>3</sub>                    | —                                                | —              | 254 nm                           | 4 h      | 1.5%         | Ir <sup>3+</sup>                   | 64   |
| Pd–Bi                                                             | Bi(NO <sub>3</sub> ) <sub>3</sub>    | PVP                                              | —              | UV                               | 0.5–3 h  | 2.86 wt%     | Bi <sup>0</sup>                    | 65   |
| Ni <sub>1</sub> /Cds                                              | Ni(CH <sub>3</sub> COO) <sub>2</sub> | —                                                | —              | UV                               | 20 min   | 2.85 wt%     | Ni(OH) <sub>2</sub>                | 66   |
| n-Cu/BP                                                           | Cu(Ac) <sub>2</sub>                  | —                                                | H <sub>2</sub> | λ > 400 nm                       | 3 h      | 11.3 wt%     | Cu <sup>δ+</sup> (0 < δ < 2)       | 67   |
| N–Co/BP                                                           | Co(Ac) <sub>2</sub>                  | —                                                | —              | —                                | —        | 5.2 wt%      | Co <sup>δ+</sup> (0 < δ < 2)       | 68   |

reaction only atomically dispersed species were active. From the viewpoint of the catalyst preparation, cyanide leaching is intricate, dangerous, and wasteful of the Au, and so, not aligned with the initial purpose of preparing atomically dispersed catalysts. Also, aggregation after the water–gas shift (WGS) reaction was observed (Fig. 3b).

The next milestone for the photochemical method was performed on a large surface-area support to increase the metal loading, while using surface ligands to stabilize the atomically dispersed species. In 2016, Liu and Zheng *et al.* reported the synthesis of a Pd<sub>1</sub>/TiO<sub>2</sub>(B) system.<sup>43</sup> Ultrathin titanium dioxide nanosheets [TiO<sub>2</sub>(B)] were used as the support. H<sub>2</sub>PdCl<sub>4</sub> was subsequently added to an aqueous dispersion of the nanosheets for the adsorption of Pd species. The mixture was then exposed to low-intensity UV light for 10 min to obtain a Pd<sub>1</sub>/TiO<sub>2</sub>(B) catalyst, as shown in Fig. 3c.

The atomic dispersion of Pd over TiO<sub>2</sub>(B) was evidenced by STEM-EDS, XAS, and AC-HAADF-STEM analyses (Fig. 3d–g). The Pd loading reached as high as 1.5 wt%, on account of the presence of surface ethylene glycolate ligands, which will be discussed below. Furthermore, this strategy enabled the continuous production of atomically dispersed Pd using a peristaltic pump and low-intensity ultraviolet irradiation in a continuous stream. Later on, the same authors found that the method was also feasible using other TiO<sub>2</sub> supports, such as anatase and commercial P25.<sup>44</sup>

Other supports could also be used for supporting single Pd atoms through liquid-phase photodeposition. Using CeO<sub>2</sub> with different morphologies, Wang *et al.* managed to reduce H<sub>2</sub>PdCl<sub>4</sub> to atomically dispersed Pd with photogenerated electrons on the surface of CeO<sub>2</sub>.<sup>49</sup> Liu *et al.* used EG–BiOBr as the support to fabricate single Pd sites with an unsaturated coordination environment.<sup>50</sup> This strategy notably boosted the N<sub>2</sub> adsorption capacity of the catalyst and thus elevated its efficiency in photocatalytic nitrogen fixation. Lu *et al.* prepared a Pd<sub>SA+C</sub>/SAPO-31 catalyst that contained Pd single atoms and clusters.<sup>51</sup> They demonstrated that the catalyst performed

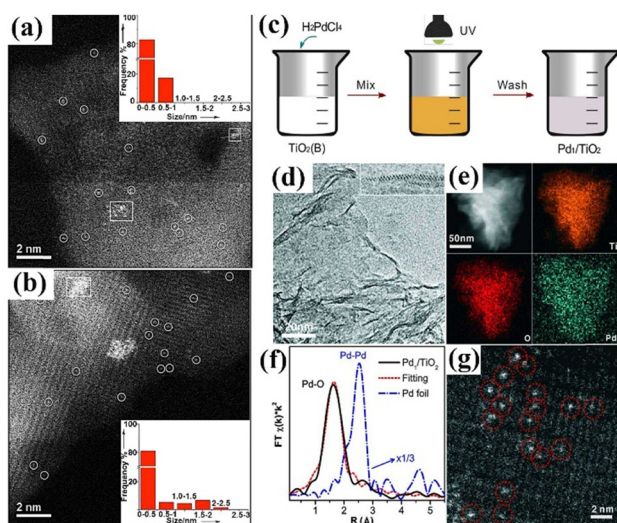


**Fig. 3** AC-HAADF/STEM images of (a) fresh 1.16 AuG5\_UV\_L and (b) used 1.16 AuG5\_UV\_L after reaction in the TPSR mode at 373 K and held steady for 4 h. Reprinted with permission.<sup>26</sup> Copyright 2013, American Chemical Society. (c) Scheme for the synthesis and (d)–(g) structural characterizations of Pd<sub>1</sub>/TiO<sub>2</sub>(B), in which (d) is a representative TEM image, (e) STEM-EDS elemental mapping, (f) FT-EXAFS spectra and (g) high-resolution HAADF-STEM image. Copyright 2016, Reprinted with permission from AAAS.<sup>27</sup>



better than the wet impregnation method-made Pd<sub>SA</sub>/SAPO-31 catalyst in the chemoselective hydrodeoxygenation of vanillin. More recently, Chen *et al.* obtained atomically dispersed and stable Pd<sub>1</sub>/TiO<sub>2</sub> catalysts by UV treatment of an acetonitrile dispersion of TiO<sub>2</sub> (anatase) and H<sub>2</sub>PdCl<sub>4</sub>, and then expanded the approach to a range of carriers (CeO<sub>2</sub> and WO<sub>3</sub>) and metal atoms (Ir, Pt, Rh, and Ru).<sup>46</sup>

Atomically dispersed Pt could also be obtained through photodeposition.<sup>68</sup> A catalyst containing atomically dispersed Pt was produced by Qiao *et al.* via the UV irradiation of a mixed aqueous solution of chloroplatinic acid and a TiO<sub>2</sub>(B) dispersion.<sup>53</sup> The obtained powder was calcined at 350 °C to remove the protective agent, to allow studying the strong metal–support interaction (SMSI) single-atom catalysis. Shi *et al.* employed ZnIn<sub>2</sub>S<sub>4</sub> as the carrier of an atomically dispersed Pt catalyst for boosting photocatalytic hydrogen production.<sup>55</sup> Liu *et al.* prepared a RuCeO<sub>x</sub> mixed oxide by a co-precipitation method and used it as a support. In their system, the photo-generated electrons generated in CeO<sub>2</sub> transferred to RuO<sub>2</sub>, so that Pt atoms could be selectively deposited on the surface of RuO<sub>2</sub>, as shown in Fig. 4a.<sup>56</sup> Fourier-transform extended X-ray absorption fine structure (EXAFS) analysis revealed the local atomic structure of Pt atoms in the samples, as shown in Fig. 4b. The Pt in Pt/RuCeO<sub>x</sub>-PA prepared photochemically was found to be uniformly distributed in a Pt–O–Ru structure, whereas Pt/RuCeO<sub>x</sub>-CA prepared by chemical activation and Pt/RuCeO<sub>x</sub>-TA prepared by thermal activation existed in a variety of Pt-bonding units, suggesting that Pt in Pt/RuCeO<sub>x</sub>-PA was loaded only on RuO<sub>2</sub>. Furthermore, the high-angle annular dark-field scanning transmission electron microscopy (HAADF-STEM) images (Fig. 4c and d) also confirmed that the isolated Pt atoms (marked with yellow circles) were selectively deposited on the RuO<sub>2</sub> side. This case showed the advantage of photochemical synthesis in comparison to the conventional wet impregnation method to direct the deposition of precious metals, through the utilization of the band structure or heterojunction structures. The photodeposition of non-noble metals as single atoms was also reported; for instance, atomically dispersed Bi on icosahedral Pd nanocrystals, single Cu and Co atoms on black phosphorus, and single Ni atoms on the surface of Cds.<sup>65–67</sup>

Liquid-phase photochemical synthesis enables reduced energy consumption and waste generation compared to conventional synthesis methods. However, specific types of supports are needed for the method, which limits its universality. Besides, the method also appears to be quite simple and straightforward. However, the real chemical reactions that occur during the photodeposition remain unclear, please see Part 4.1 for details.

### 3.2. Solid-phase photochemical synthesis

In liquid-phase photochemical reduction, the solution of a metal precursor subjected to direct UV irradiation is easily converted to a dispersion of metal nanoparticles (in the absence of supports), owing to the diffusion, aggregation, and nucleation of atoms.<sup>69</sup> Thus, for the purpose of forming single

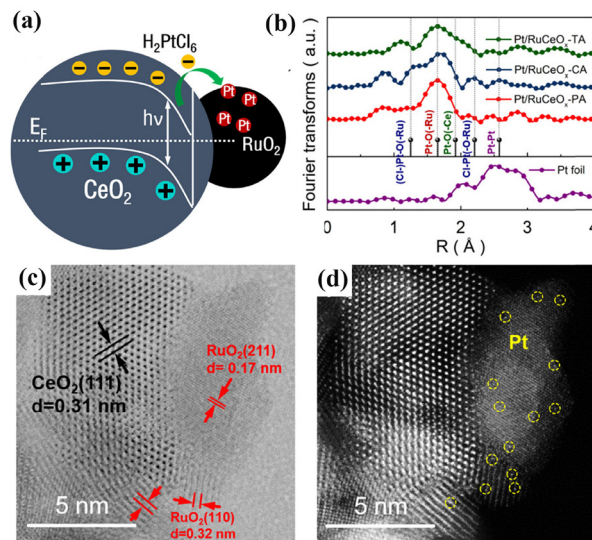


Fig. 4 (a) Schematic diagram showing the photogenerated charge separation by an internal electric field at the RuO<sub>2</sub>/CeO<sub>2</sub> heterojunction and the incorporation of platinum atoms on RuCeO<sub>x</sub>; (b) Fourier transforms of the EXAFS spectra at the Pt L<sub>3</sub>-edge for Pt/RuCeO<sub>x</sub>-TA, Pt/RuCeO<sub>x</sub>-CA, and Pt/RuCeO<sub>x</sub>-PA catalysts and Pt foil; (c) bright-field and (d) dark-field images of Pt/RuCeO<sub>x</sub>-PA (atomic Pt atoms are circled in yellow). Reproduced with permission.<sup>40</sup> Copyright 2020, Wiley-VCH.

atoms, the task is to avoid atom diffusion and metal core formation, as nucleation of the metal clusters should be avoided. To this end, solid-phase photochemical synthesis was developed, mainly through the pre-adsorption of precursors onto solid supports, or through low-temperature irradiation. Some atomically dispersed catalysts prepared by this method are summarized in Table 2.

Li *et al.* used nitrogen-doped carbon (NPC) to adsorb [PtCl<sub>6</sub>]<sup>2-</sup> ions and irradiated the obtained powder with a certain intensity of ultraviolet light to form an atomically dispersed Pt catalyst with 3.8 wt% loading (Fig. 5).<sup>70</sup> AC-STEM and XAS confirmed that the isolated Pt atoms were uniformly dispersed on the carbon at the atomic level and bonded with N atoms, as shown in Fig. 5c–f. This method can effectively avoid the agglomeration of isolated Pt atoms during the process of washing and drying. The key to this method is the uniform adsorption of metal ions in the wet impregnation step. Ligand exchange may also happen during the adsorption.

To avoid nucleation, an iced-photochemical reduction strategy was developed by Wu *et al.*, opening up new possibilities of frozen photochemistry.<sup>71</sup> In this strategy, before exposing the metal precursor to UV, the solution was rapidly frozen by liquid nitrogen (Fig. 6a). The effectiveness of the ice lattice in limiting the diffusion of reactant ions and products allowed the production of confined single atoms, that later melted into an atomic dispersion of metal atoms within the solution. The first-principles molecular dynamics (FPMD) suggested that the produced metal atoms in aqueous solution were coordinated, as H–Pt–OH, by dissociating water molecules. As illustrated in Fig. 6b–h, atomically dispersed Pt could be loaded uniformly and stably on several substrates, except for the graphene support. Additionally, the



Table 2 Summarized experimental conditions for the solid-phase photochemical syntheses of reported atomically dispersed catalysts

| Metal/support                                   | Precursor                                                                                                                | Ligand             | Reagent                                                      | Light source                          | Exposure | Content    | Valence state                       | Ref. |
|-------------------------------------------------|--------------------------------------------------------------------------------------------------------------------------|--------------------|--------------------------------------------------------------|---------------------------------------|----------|------------|-------------------------------------|------|
| Pt <sub>1</sub> /MC                             | H <sub>2</sub> PtCl <sub>6</sub>                                                                                         | —                  | —                                                            | UV/0.89 mW cm <sup>-2</sup>           | 1 h      | 2.6 wt%    | Pt <sup>δ+</sup> (1 < δ < 2)        | 71   |
| Pt/C <sub>3</sub> N <sub>4</sub>                | H <sub>2</sub> PtCl <sub>6</sub>                                                                                         | —                  | —                                                            | 420 nm/300 W Xe lamp                  | 3 min    | 3.45 wt%   | Pt <sup>δ+</sup> (δ < 4)            | 72   |
| Pt-Ru/C <sub>3</sub> N <sub>4</sub>             | H <sub>2</sub> PtCl <sub>6</sub> + RuCl <sub>3</sub>                                                                     | —                  | —                                                            | 420 nm/300 W Xe lamp                  | 10 min   | 0.51 wt%   | Pt <sup>0</sup>                     | 73   |
|                                                 |                                                                                                                          |                    |                                                              |                                       |          | 0.45 wt%   | Ru <sup>0</sup>                     |      |
| Pd/C <sub>3</sub> N <sub>4</sub>                | PdCl <sub>2</sub> /[PdCl(C <sub>3</sub> H <sub>5</sub> ) <sub>2</sub> ]/H <sub>12</sub> N <sub>6</sub> O <sub>6</sub> Pd | —                  | —                                                            | 400–780 nm/300 W Xe lamp              | 1 h      | 0.2855 wt% | Pd <sup>δ+</sup> (0 < δ < 2)        | 74   |
| Pt@HG                                           | H <sub>2</sub> PtCl <sub>6</sub>                                                                                         | —                  | C <sub>12</sub> H <sub>8</sub> N <sub>2</sub> O <sub>4</sub> | Xe lamp                               | 1 h      | 2.4%       | Pt <sup>δ+</sup> (0 < δ < 4)        | 75   |
| Ir/Ni <sub>9</sub> FeOOH                        | IrCl <sub>3</sub> (H <sub>2</sub> O) <sub>3</sub>                                                                        | —                  | —                                                            | 0.7 mW cm <sup>-2</sup>               | 1 h      | 2.99 wt%   | Ir <sup>5.3+</sup>                  | 76   |
| Pt <sub>1</sub> /CuO-CeO <sub>2</sub>           | H <sub>2</sub> PtCl <sub>6</sub>                                                                                         | —                  | —                                                            | 300 W Xe lamp/300 mW cm <sup>-2</sup> | 15 min   | 0.2 wt%    | Pt <sup>2+</sup> + Pt <sup>4+</sup> | 77   |
| Pd <sub>1</sub> /TiO <sub>2</sub>               | K <sub>2</sub> PdCl <sub>4</sub>                                                                                         | —                  | —                                                            | 300 W Xe lamp                         | 5 min    | 0.53 wt%   | Pd <sup>0</sup>                     | 78   |
| Ru/TiO <sub>2</sub>                             | RuCl <sub>3</sub>                                                                                                        | —                  | Methanol                                                     | solar light/50 W m <sup>-2</sup>      | 2 h      | 0.42 wt%   | Ru <sup>δ+</sup> (0 < δ < 4)        | 79   |
| Pt <sub>1</sub> /NMC                            | H <sub>2</sub> PtCl <sub>6</sub>                                                                                         | —                  | Ethanol                                                      | 365 nm/0.89 mW cm <sup>-2</sup>       | 1 h      | 2.54%      | Pt <sup>0</sup>                     | 80   |
| Au <sub>1</sub> /In <sub>2</sub> O <sub>3</sub> | PNSs                                                                                                                     | HAuCl <sub>4</sub> | —                                                            | λ = 253.7 nm/0.6 mW cm <sup>-2</sup>  | 1 h      | 0.51 wt%   | Au <sup>δ+</sup> + Au <sup>0</sup>  | 81   |
| Pt/NPC                                          | H <sub>2</sub> PtCl <sub>6</sub>                                                                                         | —                  | —                                                            | UV                                    | 1 h      | 3.8 wt%    | Pt <sup>0</sup>                     | 70   |
| Ag/g-C <sub>3</sub> N <sub>4</sub>              | AgNO <sub>3</sub>                                                                                                        | —                  | —                                                            | 250 W Hg lamp                         | 1 h      | 3.0 wt%    | Ag <sup>0</sup>                     | 82   |

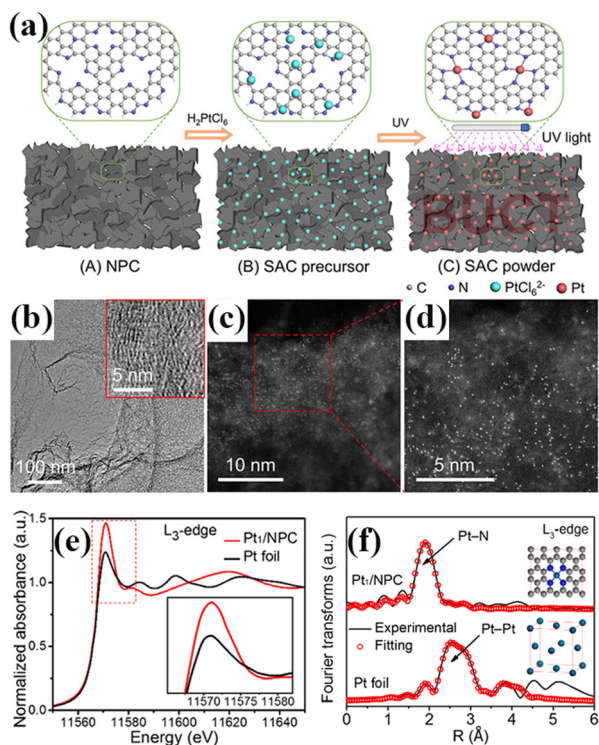


Fig. 5 (a) Schematic illustration of the formation of the Pt<sub>1</sub>/NPC catalyst; (b) HRTEM image of the Pt<sub>1</sub>/NPC catalyst; insets show enlarged (c) HADDF-STEM and (d) Pt<sub>1</sub>/NPC catalyst images; (e) normalized XANES spectra at the Pt L<sub>3</sub>-edge for the Pt<sub>1</sub>/NPC catalyst and Pt foil; (f) Fourier transform of the EXAFS spectra at the Pt L<sub>3</sub>-edge and corresponding R-space fitting curves for the Pt<sub>1</sub>/NPC catalyst and Pt foil. The insets show the atomic structure models for the Pt<sub>1</sub>/NPC and Pt foil. Reprinted with permission from ref 54. Copyright 2018 American Chemical Society.

same method was applied to form isolated Ag and Au atoms on an ultrathin carbon film (Fig. 6i and j). XANES of the Pt single-atom materials (Pt<sub>1</sub>/MC and Pt<sub>1</sub>/TiO<sub>2</sub>) also confirmed the isolated states of Pt atoms (Fig. 6k and l).

Combining the above-mentioned two solid-phase strategies, *i.e.*, pre-absorption of the metal precursor and frozen photochemical treatment, Guo *et al.* mixed a solution of the metal

precursor and dispersion of the support, then rapidly froze the mixture in liquid nitrogen and carried out UV treatment on it at 420 nm.<sup>72</sup> An atomically dispersed Pt catalyst on g-C<sub>3</sub>N<sub>4</sub> with a metal loading of 3.45 wt% was obtained. The strong coordination bonds allowed high stability at high loading. The presence of Pt–C bonds were proposed based on the EXAFS results, which we tend to disagree with.

Recently, Xu *et al.* studied the applicability of the frozen photochemical method using three distinct Pd precursors (PdCl<sub>2</sub>, [PdCl(C<sub>3</sub>H<sub>5</sub>)<sub>2</sub>], H<sub>12</sub>N<sub>6</sub>O<sub>6</sub>Pd).<sup>74</sup> The produced catalysts showed no relevance between the photocatalytic hydrogen production performance and the precursor choice. Some reports on the use of the frozen photochemical method for

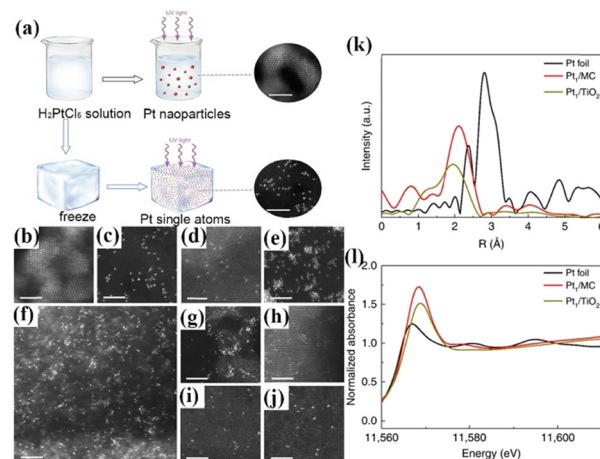


Fig. 6 (a) Schematic illustration of the iced-photochemical process; (b)–(g) HAADF-STEM images of Pt species over different supports, with (b) Pt nanocrystals with a size of ~2 nm formed by the normal photochemical reduction of H<sub>2</sub>PtCl<sub>6</sub> aqueous solution; (c) Pt single atoms dispersed on an ultrathin carbon film. (d) Densely and homogeneously dispersed Pt single atoms on mesoporous carbon; (e) Pt<sub>1</sub>/MWCNTs, indicating that Pt existed completely as isolated single atoms; (f) Pt<sub>1</sub>/graphene with concomitant Pt single atoms, nanoclusters, and sub-nanometre clusters. (g) Atomically dispersed Pt on titanium oxide nanoparticles; (h) Pt single atoms attached on the surface of zinc oxide nanowires; (i) Ag and (j) Au single atoms prepared by a similar iced-photochemical route. (scale bar, 2 nm); (k) EXAFS spectra of bulk Pt foil and Pt single atoms absorbed on TiO<sub>2</sub> and MC. (l) Normalized XANES structure spectra at the Pt L<sub>3</sub>-edge.<sup>55</sup> Open access.



loading atomically dispersed metals onto oxides are also listed in Table 2.

Solid-phase photochemical deposition is generally highly selective, preventing side reactions, like aggregation. However, the limited availability of photochemical reactions at the solid-phase surfaces can lower the reaction rate. Solid-phase synthesis usually needs a longer duration of irradiation.

### 3.3. Process control in photochemical synthesis

In this part, we discuss the controlling factors that can impact the photochemical synthesis of atomically dispersed catalysts, from the aspects of both fundamental interests and practical potential.

**3.3.1. Supports.** The supports of supported catalysts are highly important in stabilizing the active species, in activating the supported species, and in ensuring the recyclability of the whole catalysts. Some supports may even directly participate in catalytic reactions, being the active sites.<sup>45</sup> The supports of atomically dispersed catalysts are even more important in these mentioned roles, considering the high surface energy and high mobility of single atoms.<sup>1</sup> Therefore, it is crucial to select a suitable support for atomically dispersed catalysts.

The choice of supports should be adapted to the preparation methods. In photochemical synthesis, the support choice is usually limited to semiconductors; for instance TiO<sub>2</sub>, CeO<sub>2</sub>, or C<sub>3</sub>N<sub>4</sub>. Still, the structural parameters of the supports are too many to be fully studied and reported here.

First, the polymorphism of inorganic matter is the most commonly considered parameter. Our previous research demonstrated that photochemically prepared Pd<sub>1</sub>/TiO<sub>2</sub> catalysts utilizing two different types of TiO<sub>2</sub> supports, namely (001)-exposed anatase and P25, exhibited distinct CO oxidation performances despite their same degrees of atomic dispersion.<sup>45</sup> Zhang *et al.* used a newly developed 1T'-phase MoS<sub>2</sub> crystal as a support to produce an atomically dispersed Pt catalyst by a photochemical method, with a Pt loading capacity of up to 10 wt%.<sup>83</sup> Although the support was not a free-standing material, the method could still be viewed as a solid-phase photochemical synthesis. The HAADF-STEM image and simulated STEM images revealed three types of atomically dispersed Pt: Pt<sub>sub</sub>, Pt<sub>ads-S</sub>, and Pt<sub>ads-Mo</sub>. However, using 2H-phase MoS<sub>2</sub> as the support only led to the epitaxial growth of platinum (Pt) nanoparticles. In this case, the preferential enrichment of photogenerated carriers onto different facets of different crystal phases was nicely demonstrated. The morphologies of the crystalline supports also have a significant impact on the dispersion and catalytic activity of single atoms. Wang *et al.* described the photochemical synthesis of atomically dispersed Pd/CeO<sub>2</sub> catalysts with two different morphologies of CeO<sub>2</sub> (Fig. 7).<sup>49</sup> Pd/CeO<sub>2</sub>-TOP (truncated octahedral CeO<sub>2</sub>) exhibited higher activity in CO oxidation and better selectivity in the selective oxidation of benzyl alcohol than Pd/CeO<sub>2</sub>-CP (cubic CeO<sub>2</sub>), although they had similar structures of Pd, as shown in Fig. 7g and h. Pd/CeO<sub>2</sub>-TOP exposed a larger number of (111) surfaces, while the higher coordination number of Ce–O<sub>L</sub> (O<sub>L</sub>: surface lattice oxygen atoms) for cerium atoms on the CeO<sub>2</sub>(111) surface could facilitate the reaction by hydrogen removal from Pd.

For crystalline supports, the surface structures are inevitably different from the bulk structure, being a class of symmetry

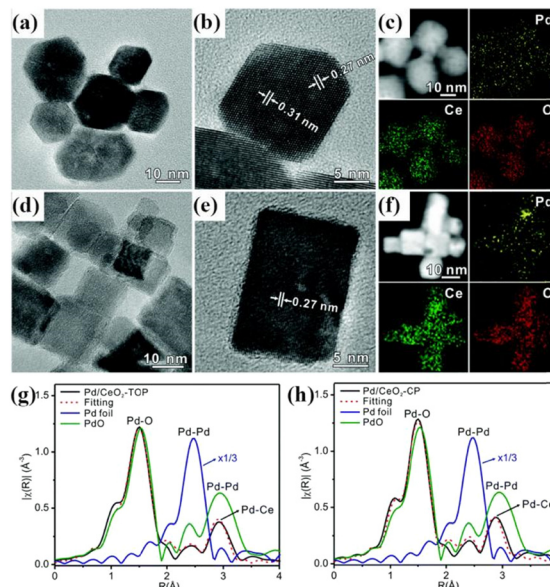


Fig. 7 (a) and (d) TEM and (b) and (e) HRTEM images of Pd/CeO<sub>2</sub>-TOP and Pd/CeO<sub>2</sub>-CP prepared via a photochemical route. (c) and (f) HAADF-STEM images of Pd/CeO<sub>2</sub>-TOP and Pd/CeO<sub>2</sub>-CP, and their corresponding EDX mappings of Pd, Ce, and O; Fourier transforms of EXAFS spectra for (g) Pd/CeO<sub>2</sub>-TOP and (h) Pd/CeO<sub>2</sub>-CP as well as the reference materials Pd foil and PdO at the Pd K-edge. Reproduced with permission.<sup>33</sup> Copyright 2017, The Royal Society of Chemistry.

breaking. The undercoordinated sites and non-stoichiometric composition, usually called defects, are beneficial for anchoring single atoms.<sup>84</sup> Wei *et al.* discovered that atomically dispersed Pt could be firmly attached to the support's edge or at a defect location on the surface of amorphous carbon film, mesoporous carbon (MC), multi-walled carbon nanotubes (MWCNTs), TiO<sub>2</sub> nanoparticles, and ZnO nanowires due to their abundant presence of defects.<sup>71</sup>

**3.3.2. Ligands.** Although usually overlooked, the presence of small coordination molecules (ligands) on the surface of supported single atoms is unquestionably true.<sup>85</sup> The origin of surface ligands is multiple: the solvent molecules (in liquid-phase synthesis), oxygen and water molecules in air, and ligands from the surface of the supports, to name a few. The ligands lower the surface energy of single atoms, and thus also stabilize them. In some cases, ligands can tune the overall catalytic performance.

Liu and Zheng *et al.* found that ethylene glycol ligands on the surface of TiO<sub>2</sub>(B) played a decisive role in the photochemical reaction process during the preparation of atomically dispersed Pd<sub>1</sub>/TiO<sub>2</sub>(B).<sup>43</sup> As shown in Fig. 8a, when the support was exposed to ultraviolet light, electron-hole pairs were generated. The electrons were trapped in the Ti-3d orbital to form the Ti<sup>3+</sup> site (detected), while the holes broke the Ti–O bond between the glycolate and TiO<sub>2</sub>, resulting in the formation of the –OCH<sub>2</sub>CH<sub>2</sub>O• radical. A hydrogen transfer occurred between α-H and –OCH<sub>2</sub>CH<sub>2</sub>O• to form –OCH<sub>2</sub>•CHOH radicals (detected). Once PdCl<sub>4</sub><sup>2-</sup> was adsorbed on TiO<sub>2</sub>(B), each PdCl<sub>4</sub><sup>2-</sup> released two Cl<sup>-</sup> ions, producing an intermediate with a separate PdCl<sub>2</sub>



unit adsorbed on  $\text{TiO}_2(\text{B})$ . Subsequently, the  $-\text{OH}$  group in  $-\text{OCH}_2\cdot\text{CHOH}$  attacked the Pd site nearby by substituting one  $\text{Cl}^-$  to form a  $\text{PdCl}_1/\text{TiO}_2$  intermediate. Finally, the residual  $\text{Cl}^-$  on  $\text{PdCl}_1/\text{TiO}_2$  could be easily removed by  $\text{H}_2$  treatment to generate  $\text{H}^+$  and  $\text{Cl}^-$ . Overall, EG radicals promoted the removal of  $\text{Cl}^-$  on Pd and stabilized the isolated Pd atoms by forming more Pd-O bonds. More importantly, the formed Pd-EG-TiO<sub>2</sub> interface facilitated the heterolytic activation of  $\text{H}_2$ , thus improving the catalytic hydrogenation performance, especially in the hydrogenation of polar bonds. Without surface EG ligands, the loading of metal would not exceed 1 wt%, meanwhile the catalytic hydrogenation performance would be lower. The EG-protected  $\text{TiO}_2(\text{B})$  was utilized to synthesize several other atomically dispersed catalysts.<sup>47,53,79</sup>

Very recently, Chen *et al.* synthesized an atomically dispersed  $\text{Pd}_1/\text{TiO}_2$  (commercial anatase) catalyst using a photochemical method in acetonitrile (Fig. 8b).<sup>46</sup> Acetonitrile was believed to be activated by oxygen vacancies on  $\text{TiO}_2$  and then ultraviolet light. The alkyl radical generated by light reacted with  $[\text{PdCl}_4]^{2-}$  ions to dissociate  $\text{Cl}^-$  ions, with the N atom and the lattice oxygen on N/TiO<sub>2</sub> serving as anchoring sites for the Pd atom. The role of acetonitrile in this system resembled that of ethylene glycol in the  $\text{Pd}_1/\text{TiO}_2(\text{B})$  system. Its primary function was to produce radicals that eliminate  $\text{Cl}^-$  with the aid of light, thereby dispersing and stabilizing the Pd atoms.

In a photochemical synthesis of an atomically dispersed  $\text{Ni}_1/\text{CdS}$  catalyst, Zhang *et al.* discovered the significant involvement of hydroxyl groups on the surface of CdS.<sup>66</sup> Fig. 8c



**Fig. 8** (a) Energies and models of the intermediates and transition states in the stepwise preparation mechanism of  $\text{Pd}_1/\text{TiO}_2(\text{B})$ . From ref. 27. Reprinted with permission from AAAS. (b) Schematic illustrating the photochemical process, and energies and optimized structures in the anchoring process of Pd single atoms in  $\text{TiO}_2$ . Reproduced with permission.<sup>50</sup> Copyright 2023, Wiley-VCH. (c) Schematic illustration of the preparation of  $\text{Ni}_1/\text{CdS}$  by a photochemical method. Reprinted from Publication ref. 50. Copyright 2020, with permission from Elsevier. (d) Schematic illustration of the preparation of Pt-SA@HG, Pt-Clu@HG, and Pt-Nc@HG. Reproduced with permission.<sup>59</sup> Copyright 2022, Wiley-VCH. (e) Illustration of the synthesis of Pt-PVP/TNR@GC catalysts, and change in the local structure of a Pt atom coordinated by PVP before and after UV irradiation.<sup>41</sup> Open access.





illustrates how CdS gets excited by light, resulting in the formation of electron-hole pairs. Thiourea acts as a sacrificial agent and consumes the holes while the electrons reduce hydrogen ions to H<sub>2</sub>. The residual hydroxyl ions react with adsorbed Ni<sup>2+</sup> to yield isolated Ni(OH)<sub>2</sub> species. We believe the coordination role of S in the support should not be overlooked. Sun *et al.* absorbed 2,2'-bipyridine-4,4'-dicarboxylic acid (C<sub>12</sub>H<sub>8</sub>N<sub>2</sub>O<sub>4</sub>) ligands onto reduced graphene through electrostatic interaction to anchor Pt ions, and subsequently transformed the structure into Pt-C coordination structures by heat treatment.<sup>75</sup> In contrast, in the absence of associated ligands, Pt tended to form clusters, as illustrated in Fig. 8d.

To prevent the aggregation of Pt atoms during photochemical reduction, Li *et al.* employed pyrrolidone (PVP) as an organic ligand and fixed it to TNR@GC (graphite-carbon encapsulated titanium oxide nanorods) *via* van der Waals forces (as depicted in Fig. 8e).<sup>57</sup> Under ultraviolet radiation, the PVP side chains tended to form stable complexes with photoreduced Pt atoms. This coordination could effectively hinder the aggregation of isolated Pt atoms, allowing a Pt loading of up to 1.75 wt%. The coordination between partially positively charged Pt atoms and amide groups (N-C=O) in PVP molecules served as the active centres for the hydrogen production reaction (HER).

**3.3.3. Sacrificial agent.** Sacrificial agents are commonly employed in the photodeposition of nanoparticles and significantly influence the synthesis.<sup>39</sup> The traditional classification of sacrificial agents falls into two main groups: electron donors and hole donors, which are added to prevent the recombination of photogenerated electron-hole pairs.<sup>86</sup> Some other types of reagents can also be viewed as sacrificial agents, for instance photosensitizers, as they would not interfere in the photoreactions after the generation of carriers.

Similarly, sacrificial agents are often used in the photochemical preparation of atomically dispersed catalysts. Maria *et al.* emphasized the necessity of adding ethanol as an electron acceptor to prepare isolated Au species.<sup>42</sup> Otherwise, gold ions would be quickly reduced in H<sub>2</sub>O<sub>2</sub> or H<sub>2</sub>O solutions and grow into metal particles. Li *et al.* used ethanol in the preparation of the Pt-PVP/TNR@GC catalyst to eliminate photogenerated holes.<sup>57</sup> Wenderich *et al.* discovered that methanol could generate methyl radicals, hence improving the reducing ability of Pt ions during the photodeposition process.<sup>87</sup> Additionally, to suppress photogenerated electron-hole recombination, thiourea and triethanolamine (TEOA) are frequently used as hole scavengers.<sup>66,88,89</sup>

It is noteworthy that careful selection of the sacrificial agents is crucial in the photochemical preparation of atomically dispersed catalysts, as they can often accelerate the deposition rate of metal ions and may lead to agglomeration.<sup>63</sup> Besides, added reagents generally serve multiple purposes in one system, which makes it difficult to understand the photochemical reaction.

Environment-unfriendly sacrificial agents should be avoided. The price of sacrificial agent should not be overlooked too for industrial considerations. Apart from the commonly used alcohols, it is also worth considering novel sacrificial agents for photocatalytic hydrogen production, including biomass and

plastic waste, which might also be used to synthesize atomically dispersed catalysts using photochemical techniques.

**3.3.4. Light source.** Regarding the only energy input needed for photochemical synthesis, the choice of light source needs to be considered under different conditions: (1) when the support is a semiconductor, the photon energy of the incident light must surpass the band gap energy of the semiconductor, so that photocarriers can be generated; (2) when the support is absent during photoirradiation (for instance in frozen photosynthesis), the light source needs to provide enough energy to decompose the metal precursor. Accordingly, selecting light sources with an appropriate wavelength and intensity is crucial to achieve efficient photochemical synthesis. Nonetheless, it should not be assumed that the larger the light's energy, the better the results.

Gold ions can be readily reduced with visible light.<sup>90</sup> To form atomically dispersed Au, it is necessary to either employ an appropriate excitation wavelength or add a sacrificial agent.<sup>42</sup> Zhou *et al.* used UV excitation at a wavelength of 420 nm to avoid the direct reduction of [PtCl<sub>6</sub>]<sup>2-</sup> into nanoparticles.<sup>72</sup> This method involved selectively exciting electrons solely at the g-C<sub>3</sub>N<sub>4</sub> defect sites, which ensured that only Pt ions adsorbed on the surface could be reduced. This approach could effectively prevent detrimental Pt growth. Our previous work used the 365 nm light of a Xenon lamp, which was weak enough to prevent the photodegradation of surface EG ligands, but strong enough to allow the formation of EG radicals to anchor Pd single atoms.<sup>43</sup>

**3.3.5. Temperature.** The crucial aspect of producing atomically dispersed catalysts *via* a photochemical technique is to impede the further nucleation and aggregation of single atoms during the reaction process. The activation energy of nucleation has a close correlation with the reaction temperature. Li *et al.* compared the photodeposition process at three temperatures (0 °C, 25 °C, and 60 °C) and observed that as the temperature increased, Pt nanoparticles deposited on the TiO<sub>2</sub> surface gradually grew from a highly dispersed state (2.9 nm) to large particles exceeding 20 nm.<sup>91</sup> Wei *et al.* froze a mixed ethanol and water solution of a metal precursor to -60 °C and then conducted photoreduction.<sup>80</sup> At this temperature, they obtained an atomically dispersed Pt catalyst, unlike the Pt nanoparticle obtained under room temperature reduction.

### 3.4. Catalytic applications

Atomically dispersed catalysts prepared *via* photochemical synthesis have shown unique functions in several catalytic processes.

**3.4.1. Photocatalysis.** Catalysts prepared this way commonly have a strong capability for light absorption due to the choice of support. Besides, photodeposition was developed to improve the photocatalytic performances of semiconductors in the first place. Hence, photocatalysis is a valid application.<sup>92</sup> To name a few examples, Ni<sub>1</sub>/CdS,<sup>66</sup> Pt<sub>1</sub>/ZnIn<sub>2</sub>S<sub>4</sub>,<sup>55</sup> and Pt<sub>1</sub>/g-C<sub>3</sub>N<sub>4</sub><sup>72</sup> have been reported for photocatalytic hydrogen evolution (HER), while Pd-EG-BiOBr<sup>50</sup> and Ru<sub>1</sub>/TiO<sub>2</sub><sup>79</sup> have been reported for photocatalytic N<sub>2</sub> fixation. In the case of Pt<sub>1</sub>/h-ZIS



(Fig. 9), the hexagonal  $\text{ZnIn}_2\text{S}_4$  (h-ZIS) nanosheets offered uniform S3 sites to anchor Pt single atoms, forming a Pt-S3 tetrahedral coordination structure that could effectively prevent electron-hole pair recombination and produce tip effects *via* proficient proton mass transfer, which would enhance the adsorption/desorption action of H.

**3.4.2. Electrocatalysis.** Considering the supports used in photochemical synthesis are usually semiconductors or carbon, electrocatalysis is also commonly considered. The related work focusing on the reaction by all kinds of atomically dispersed catalysts has been nicely summarized before by others.<sup>93</sup> We list several examples here that relate to the photochemical synthetic approach: Pt over carbon,<sup>57</sup> Pt/RuCeO<sub>x</sub>,<sup>56</sup> Pt-SA@HG (HG = holey reduced graphene oxide)<sup>75</sup> and Pt<sub>1</sub>/NMC (NMC = nitrogen-doped mesoporous carbon)<sup>80</sup> for the HER and Ir-SAC<sup>76</sup> for the oxygen evolution reaction.

**3.4.3. Thermocatalysis.** Thermocatalysis is a well-recognized form of catalysis that is widely used in traditional industrial procedures, owing to its remarkable efficiency and ability for mass production. As atomically dispersed catalysts prepared from other methods, photochemically produced

catalysts should also be considered in thermocatalysis for possible industrial prospect. Reports on selective hydrogenation,<sup>43</sup> oxidation,<sup>53,73,77</sup> selective hydrodeoxygenation,<sup>51</sup> and alkoxylation and alkylation<sup>94</sup> have been published.

**3.4.4. Other applications.** Pd<sub>1</sub>/TiO<sub>2</sub> prepared by iced-photochemistry was reported to function as a photocatalytic sensing material that had high sensitivity and selectivity in detecting chlorpyrifos.<sup>78</sup> The material achieved a detection limit of 0.01 ng mL<sup>-1</sup>, well below the maximum residue limit allowed by the U.S. Environmental Protection Agency (10 ppb).

## 4. Challenges and perspective

We summarized the advantages of photochemical synthesis for atomically dispersed catalysts in the last paragraph of Part 2. We also presented many examples to show how the method is tuneable and has been well-demonstrated in different systems. Practices have proved that this approach is not only environmentally friendly and safe, but also easy to execute and holds great potential for mass production. However, the method still has several issues that need to be addressed in the future, both from the aspects of science and technology: (1) lack of fundamental understanding of the process; (2) low level of control of the structure and (3) limited number of demonstrated systems. Here, we elaborate the challenges the method faces and give suggestions for further research.

### 4.1. Lack of fundamental understanding of the process

Being a kind of wet-chemistry method, photochemical synthesis inherits both the advantages (for instance, easy scale up for mass production) and disadvantages of wet-chemistry methods. The most profound disadvantage that hinders addressing the other two issues (structure control and extension of the method) is that the basic chemical reactions, especially radical reactions, that happen in photochemical synthesis are not fully understood.

Although we point out in Part 2 that the photogenerated carriers are very likely the driving force of single-atoms' formation and stabilization, the real process has to be much more complicated than that simply laid out eqn (1) and (2). In the presence of solvent and ligands from the metal precursor, photogenerated electrons and holes on the surface can produce extensive kinds of radicals. For instance, it was reported that as many as tens of radical species could be formed in a water dispersion of TiO<sub>2</sub> upon photoirradiation.<sup>95,96</sup> These radicals may serve as the real intermediates to react with the metal precursors and lead to the photodeposition.

Another evidence on the complexity of the chemical reaction is the oxidation state of the supported metal species. Although usually called "single atoms", accompanied by the use of terms like "photoreduction" and "photoreducing", the supported single metal atoms are not likely to be zero-valenced. The major reaction in the photodeposition of metallic nanoparticles is reduction, obviously, but not in the case in photodepositing single atoms. Some reports claimed their products were composed of M<sup>0</sup> single atoms, which we tend to disagree with.

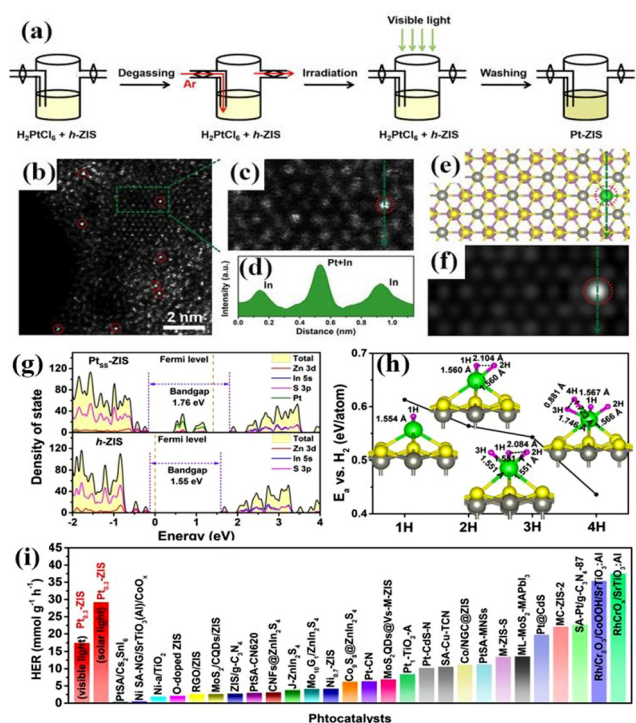


**Fig. 9** (a) Schematic of the synthesis of Pt-ZIS; (b) HAADF-STEM and (c) magnified HAADF-STEM image of Pt = ZIS. (d) Strength profiles from the areas labelled by the green line. (e) Optimized structure of Pt<sub>0.3</sub>-ZIS, where the yellow, grey, pink, and green spheres represent S, Zn, In, and Pt atoms, respectively. (f) Simulated HAADF-STEM image of Pt<sub>SS</sub>-ZIS according to the DFT-optimized structure. (g) Density of states of h-ZIS and Pt<sub>SS</sub>-ZIS. (h) Calculated adsorption energies of H atoms as a function of the H coverage (from one H atom to four H atoms) on single Pt atom photocatalysts with h-ZIS as the support. The H-H and Pt-H distances are shown in the figure; (i) H<sub>2</sub> evolution rates for Pt<sub>0.3</sub>-ZIS in this work compared with representative recently reported photocatalysts.<sup>39</sup> Open access.



The coordination bonds between single atoms and the support will lead to charge transfer, hence there will be partial charge on the metal centres (unless the metal was fully coordinated by neutral molecules, like ethene and water). Bearing this in mind, photochemical synthesis is, in principle, not a reduction reaction for the metal. In our previous reports, the supported Pd did not change its oxidation state before and after phototreatment.<sup>43</sup> The reaction was more a radical-assisted ligand exchange reaction.

With numerous factors involved in the synthesis, we believe a better understanding of the reactions in photochemical synthesis calls for a systematic study in different systems, or in well-defined model systems.

#### 4.2 Low level of control of the structure

We believe the structures of atomically dispersed catalysts need a higher level of rational design and controllable synthesis, in the following three aspects in particular:

(1) **Loading amount.** Of all the structural properties, the one that mostly hinders their application is the loading amount of metal. Reducing the concentration of the metal precursors in solution is vital to maintain an adequate distance between precipitated metal atoms to prevent their further aggregation, as the same for all wet-chemical methods. Yet, industrial reactors have limited space. A lower loading of active sites would mean a lower space-time velocity, and hence lower output.

Using high surface-area supports, like activated carbon, two-dimensional supports, or porous supports would help increase the metal loading. Using supports that can bind strongly with single metal atoms, or using surface ligands to prevent the surface diffusion is also a practical strategy.

(2) **Coordination structure.** The catalytic performances of atomically dispersed catalysts are determined by the local structures of single sites, which impact the adsorption and activation of reactants. The rational design of the local structures and preparation of a catalyst with well-defined structures is crucial, especially in comprehending the structure–activity correlation of catalysts, and in developing better catalysts.

In photochemical synthesis, not only is the surface reaction mechanism unclear, the multiple roles of possible spectators (solvents, added ligands, photogenerated radicals) are also unclear. These species may coordinate with the metal sites and even contribute in catalytic reactions. Li *et al.* found the amide group (N–C=O) in the Pt-PVP/TNR@GC catalyst was coordinated with isolated Pt atoms and donated electrons.<sup>57</sup> The partially positively charged Pt atoms located in the –C=O section of the pyrrolidone side chain were found to function as the active centre for the HER. EG ligands were found to significantly contribute to catalytic hydrogenation and photocatalytic nitrogen fixation.<sup>50</sup>

(3) **Uniformity of the coordination structure.** As we pointed out in Part 1, the uniformity of single atoms, especially in their coordination structures, is still under debate. The heterogeneity can form a complicated support surface and lead to imprecise preparation methods.<sup>97</sup> The pursuit of exploring the “structure–property” relationship with single-atom catalysts seems to

still be challenging, since the accurate molecular definition of the active sites is not easy.

Compared to conventional synthesis *via* annealing, the photochemical reaction offers gentler and more controllable reaction conditions, thereby largely preserving the supports' surface structure. In addition, it allows the selective deposition of individual atoms at desired positions on a well-defined surface, with great accuracy. Using highly crystallized materials as the support with well-defined exposed surfaces can serve as model systems to tackle this problem.<sup>83</sup> For instance, hexagonal ZnIn<sub>2</sub>S<sub>4</sub> (h-ZIS) nanosheets offer uniform S3 sites for anchoring Pt atoms *via* photochemical reactions.<sup>55</sup>

#### 4.3 Limited number of demonstrated systems

The synthesis and application of photochemically produced-atomically dispersed catalysts are both limited in several cases. To the best of our knowledge, we have summarized all the reported cases in Tables 1 and 2.

To date, the selected supports are mainly TiO<sub>2</sub>, carbon-based materials and sulfides. It is essential to evaluate the capability of other supports. It is possible to acquire the desired material by adjusting the input energy of the light source for the photochemical reaction. The limited cases of chosen supports also limit the studied catalytic reactions.

#### 4.4 Summary

As a novel technique for synthesizing atomically dispersed catalysts, the photochemical method possesses substantial promise for future research and application, but with several issues to be addressed. Since 2013 and 2016,<sup>42,43</sup> the fast development in the method has given us confidence that the future will witness an increasingly vital role of atomically dispersed catalysts prepared by photochemical methods in energy conversion, environmental protection, and new material synthesis.

## Conflicts of interest

There are no conflicts to declare.

## Acknowledgements

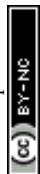
This work was supported by the ShanghaiTech University Start-up Funding and the Shanghai Pujiang Talent Program, China (No. 21PJ1410400).

## References

- X.-F. Yang, A. Wang, B. Qiao, J. Li, J. Liu and T. Zhang, Single-Atom Catalysts: A New Frontier in Heterogeneous Catalysis, *Acc. Chem. Res.*, 2013, **46**, 1740–1748.
- A. Wang, J. Li and T. Zhang, Heterogeneous single-atom catalysis, *Nat. Rev. Chem.*, 2018, **2**, 65–81.
- X. Cui, W. Li, P. Ryabchuk, K. Junge and M. Beller, Bridging homogeneous and heterogeneous catalysis by heterogeneous single-metal-site catalysts, *Nat. Catal.*, 2018, **1**, 385–397.



- 4 M. Haruta, T. Kobayashi, H. Sano and N. Yamada, Novel Gold Catalysts for the Oxidation of Carbon Monoxide at a Temperature far Below 0 °C, *Chem. Lett.*, 1987, **16**, 405–408.
- 5 G. C. Bond, The origins of particle size effects in heterogeneous catalysis, *Surf. Sci.*, 1985, **156**, 966–981.
- 6 B. Gao, K. Zhang, Y. Wang, J. Lu and P. Liu, On the Structure Insensitivity of Propane Total Oxidation over Pt/CeO<sub>2</sub>: A Comparison between Single Atoms, Clusters and Nanoparticles, *ChemCatChem*, 2023, **15**, e202301160.
- 7 B. Qiao, A. Wang, X. Yang, L. F. Allard, Z. Jiang, Y. Cui, J. Liu, J. Li and T. Zhang, Single-atom catalysis of CO oxidation using Pt<sub>1</sub>/FeO<sub>x</sub>, *Nat. Chem.*, 2011, **3**, 634–641.
- 8 S. Ding, M. J. Hülsey, J. Pérez-Ramírez and N. Yan, Transforming Energy with Single-Atom Catalysts, *Joule*, 2019, **3**, 2897–2929.
- 9 Z. Liang, J. Shen, X. Xu, F. Li, J. Liu, B. Yuan, Y. Yu and M. Zhu, Advances in the Development of Single-Atom Catalysts for High-Energy-Density Lithium–Sulfur Batteries, *Adv. Mater.*, 2022, **34**, 2200102.
- 10 Z.-H. Xue, D. Luan, H. Zhang and X. W. Lou, Single-atom catalysts for photocatalytic energy conversion, *Joule*, 2022, **6**, 92–133.
- 11 T. Cui, L. Li, C. Ye, X. Li, C. Liu, S. Zhu, W. Chen and D. Wang, Heterogeneous Single Atom Environmental Catalysis: Fundamentals, Applications, and Opportunities, *Adv. Funct. Mater.*, 2022, **32**, 2108381.
- 12 Y. Shang, X. Xu, B. Gao, S. Wang and X. Duan, Single-atom catalysis in advanced oxidation processes for environmental remediation, *Chem. Soc. Rev.*, 2021, **50**, 5281–5322.
- 13 J. Gao, L. Feng, R. Ma, B.-J. Su, A. M. Alenad, Y. Liu, M. Beller and R. V. Jagadeesh, Cobalt single-atom catalysts for domino reductive amination and amidation of levulinic acid and related molecules to N-heterocycles, *Chem. Catal.*, 2022, **2**, 178–194.
- 14 K. Sun, H. Shan, H. Neumann, G.-P. Lu and M. Beller, Efficient iron single-atom catalysts for selective ammoxidation of alcohols to nitriles, *Nat. Commun.*, 2022, **13**, 1848.
- 15 V. B. Saptal, V. Ruta, M. A. Bajada and G. Vilé, Single-Atom Catalysis in Organic Synthesis, *Angew. Chem., Int. Ed.*, 2023, **62**, e202219306.
- 16 M. Flytzani-Stephanopoulos and B. C. Gates, Atomically Dispersed Supported Metal Catalysts, *Annu. Rev. Chem. Biomol.*, 2012, **3**, 545–574.
- 17 M. Babucci, A. Guntida and B. C. Gates, Atomically Dispersed Metals on Well-Defined Supports including Zeolites and Metal-Organic Frameworks: Structure, Bonding, Reactivity, and Catalysis, *Chem. Rev.*, 2020, **120**, 11956–11985.
- 18 S. Ji, Y. Chen, X. Wang, Z. Zhang, D. Wang and Y. Li, Chemical Synthesis of Single Atomic Site Catalysts, *Chem. Rev.*, 2020, **120**, 11900–11955.
- 19 M. K. Samantaray, V. D'Elia, E. Pump, L. Falivene, M. Harb, S. Ould Chikh, L. Cavallo and J.-M. Basset, The Comparison between Single Atom Catalysis and Surface Organometallic Catalysis, *Chem. Rev.*, 2020, **120**, 734–813.
- 20 M. D. Korzyński and C. Copéret, Single sites in heterogeneous catalysts: separating myth from reality, *Trends Chem.*, 2021, **3**, 850–862.
- 21 F. Wu and P. Liu, Surface Organometallic Chemistry for Single-site Catalysis and Single-atom Catalysis, *Chem. Res. Chin. Univ.*, 2022, **38**, 1139–1145.
- 22 P. Liu and N. Zheng, Coordination chemistry of atomically dispersed catalysts, *Natl. Sci. Rev.*, 2018, **5**, 636–638.
- 23 R. Qin, K. Liu, Q. Wu and N. Zheng, Surface Coordination Chemistry of Atomically Dispersed Metal Catalysts, *Chem. Rev.*, 2020, **120**, 11810–11899.
- 24 M. J. Hülsey, S. Wang, B. Zhang, S. Ding and N. Yan, Approaching Molecular Definition on Oxide-Supported Single-Atom Catalysts, *Acc. Chem. Res.*, 2023, **56**, 561–572.
- 25 J. Resasco, L. DeRita, S. Dai, J. P. Chada, M. Xu, X. Yan, J. Finzel, S. Hanukovich, A. S. Hoffman, G. W. Graham, S. R. Bare, X. Pan and P. Christopher, Uniformity Is Key in Defining Structure–Function Relationships for Atomically Dispersed Metal Catalysts: The Case of Pt/CeO<sub>2</sub>, *J. Am. Chem. Soc.*, 2020, **142**, 169–184.
- 26 C. Jia, Q. Wang, J. Yang, K. Ye, X. Li, W. Zhong, H. Shen, E. Sharman, Y. Luo and J. Jiang, Toward Rational Design of Dual-Metal-Site Catalysts: Catalytic Descriptor Exploration, *ACS Catal.*, 2022, **12**, 3420–3429.
- 27 R. Qin, P. Liu, G. Fu and N. Zheng, Strategies for Stabilizing Atomically Dispersed Metal Catalysts, *Small Methods*, 2018, **2**, 1700286.
- 28 Z.-Y. Wu, P. Zhu, D. A. Cullen, Y. Hu, Q.-Q. Yan, S.-C. Shen, F.-Y. Chen, H. Yu, M. Shakouri, J. D. Arregui-Mena, A. Ziabari, A. R. Paterson, H.-W. Liang and H. Wang, A general synthesis of single atom catalysts with controllable atomic and mesoporous structures, *Nat. Synth.*, 2022, **1**, 658–667.
- 29 W. Guo, Z. Wang, X. Wang and Y. Wu, General Design Concept for Single-Atom Catalysts toward Heterogeneous Catalysis, *Adv. Mater.*, 2021, **33**, 2004287.
- 30 S. K. Kaiser, Z. Chen, D. Faust Akl, S. Mitchell and J. Pérez-Ramírez, Single-Atom Catalysts across the Periodic Table, *Chem. Rev.*, 2020, **120**, 11703–11809.
- 31 L. Xing, Y. Jin, Y. Weng, R. Feng, Y. Ji, H. Gao, X. Chen, X. Zhang, D. Jia and G. Wang, Top-down synthetic strategies toward single atoms on the rise, *Matter*, 2022, **5**, 788–807.
- 32 J. Wang, Z. Li, Y. Wu and Y. Li, Fabrication of Single-Atom Catalysts with Precise Structure and High Metal Loading, *Adv. Mater.*, 2018, **30**, 1801649.
- 33 N. Cheng, L. Zhang, K. Doyle-Davis and X. Sun, Single-Atom Catalysts: From Design to Application, *Electrochem. Energy Rev.*, 2019, **2**, 539–573.
- 34 F. Zhang, Y. Zhu, Q. Lin, L. Zhang, X. Zhang and H. Wang, Noble-metal single-atoms in thermocatalysis, electrocatalysis, and photocatalysis, *Energy Environ. Sci.*, 2021, **14**, 2954–3009.
- 35 Z. Li, B. Li, Y. Hu, X. Liao, H. Yu and C. Yu, Emerging Ultrahigh-Density Single-Atom Catalysts for Versatile Heterogeneous Catalysis Applications: Redefinition, Recent Progress, and Challenges, *Small Struct.*, 2022, **3**, 2200041.
- 36 W. C. Clark and A. G. Vondjidis, An infrared study of the photocatalytic reaction between titanium dioxide and silver nitrate, *J. Catal.*, 1965, **4**, 691–696.
- 37 B. Kraeutler and A. J. Bard, Heterogeneous photocatalytic preparation of supported catalysts. Photodeposition of



- platinum on titanium dioxide powder and other substrates, *J. Am. Chem. Soc.*, 1978, **100**, 4317–4318.
- 38 K. Wenderich and G. Mul, Methods, Mechanism, and Applications of Photodeposition in Photocatalysis: A Review, *Chem. Rev.*, 2016, **116**, 14587–14619.
- 39 H. Zhao, Q. Mao, L. Jian, Y. Dong and Y. Zhu, Photodeposition of earth-abundant cocatalysts in photocatalytic water splitting: Methods, functions, and mechanisms, *Chin. J. Catal.*, 2022, **43**, 1774–1804.
- 40 G. Chen, R. Li and L. Huang, Advances in photochemical deposition for controllable synthesis of heterogeneous catalysts, *Nanoscale*, 2023, **15**, 13909–13931.
- 41 J. M. Thomas, Z. Saghi and P. L. Gai, Can a Single Atom Serve as the Active Site in Some Heterogeneous Catalysts?, *Top. Catal.*, 2011, **54**, 588–594.
- 42 M. Yang, L. F. Allard and M. Flytzani-Stephanopoulos, Atomically Dispersed Au(OH)<sub>x</sub> Species Bound on Titania Catalyze the Low-Temperature Water-Gas Shift Reaction, *J. Am. Chem. Soc.*, 2013, **135**, 3768–3771.
- 43 P. Liu, Y. Zhao, R. Qin, S. Mo, G. Chen, L. Gu, D. M. Chevrier, P. Zhang, Q. Guo, D. Zang, B. Wu, G. Fu and N. Zheng, Photochemical route for synthesizing atomically dispersed palladium catalysts, *Science*, 2016, **352**, 797–800.
- 44 P. Liu, J. Chen and N. Zheng, Photochemical route for preparing atomically dispersed Pd<sub>1</sub>/TiO<sub>2</sub> catalysts on (001)-exposed anatase nanocrystals and P25, *Chin. J. Catal.*, 2017, **38**, 1574–1580.
- 45 P. Liu, Y. Zhao, R. Qin, L. Gu, P. Zhang, G. Fu and N. Zheng, A vicinal effect for promoting catalysis of Pd<sub>1</sub>/TiO<sub>2</sub>: supports of atomically dispersed catalysts play more roles than simply serving as ligands, *Sci. Bull.*, 2018, **63**, 675–682.
- 46 X. Chen, S. Guan, J. Zhou, H. Shang, J. Zhang, F. Lv, H. Yu, H. Li and Z. Bian, Photocatalytic Free Radical-Controlled Synthesis of High-Performance Single-Atom Catalysts, *Angew. Chem., Int. Ed.*, 2023, **62**, e202312734.
- 47 X.-L. Ye, S.-J. Lin, J.-W. Zhang, H.-J. Jiang, L.-A. Cao, Y.-Y. Wen, M.-S. Yao, W.-H. Li, G.-E. Wang and G. Xu, Boosting Room Temperature Sensing Performances by Atomically Dispersed Pd Stabilized via Surface Coordination, *ACS Sens.*, 2021, **6**, 1103–1110.
- 48 K. Du, M. Sun, J. Peng, S. Zhou, G. Sheng, R. Shen, L. Deng, C. Hu, Y. Sun and P. Zhang, Mixed-valence palladium single-atom catalyst induced by hybrid TiO<sub>2</sub>-graphene through a photochemical strategy, *Appl. Surf. Sci.*, 2023, **625**, 157115.
- 49 X. Wang, J. Chen, J. Zeng, Q. Wang, Z. Li, R. Qin, C. Wu, Z. Xie and L. Zheng, The synergy between atomically dispersed Pd and cerium oxide for enhanced catalytic properties, *Nanoscale*, 2017, **9**, 6643–6648.
- 50 J. Liu, F. Li, J. Lu, R. Li, Y. Wang, Y. Wang, X. Zhang, C. Fan and R. Zhang, Atomically dispersed Palladium-Ethylene Glycol- Bismuth oxybromide for photocatalytic nitrogen fixation: Insight of molecular bridge mechanism, *J. Colloid Interface Sci.*, 2021, **603**, 17–24.
- 51 X. Lu, C. Guo, M. Zhang, L. Leng, J. H. Horton, W. Wu and Z. Li, Rational design of palladium single-atoms and clusters supported on silicoaluminophosphate-31 by a photochemical route for chemoselective hydrodeoxygenation of vanillin, *Nano Res.*, 2021, **14**, 4347–4355.
- 52 M.-Y. Qi, M. Conte, Z.-R. Tang and Y.-J. Xu, Engineering Semiconductor Quantum Dots for Selectivity Switch on High-Performance Heterogeneous Coupling Photosynthesis, *ACS Nano*, 2022, **16**, 17444–17453.
- 53 B. Han, Y. Guo, Y. Huang, W. Xi, J. Xu, J. Luo, H. Qi, Y. Ren, X. Liu, B. Qiao and T. Zhang, Strong Metal-Support Interactions between Pt Single Atoms and TiO<sub>2</sub>, *Angew. Chem., Int. Ed.*, 2020, **59**, 11824–11829.
- 54 Y. Sui, S. Liu, T. Li, Q. Liu, T. Jiang, Y. Guo and J.-L. Luo, Atomically dispersed Pt on specific TiO<sub>2</sub> facets for photocatalytic H<sub>2</sub> evolution, *J. Catal.*, 2017, **353**, 250–255.
- 55 X. Shi, C. Dai, X. Wang, J. Hu, J. Zhang, L. Zheng, L. Mao, H. Zheng and M. Zhu, Protruding Pt single-sites on hexagonal ZnIn<sub>2</sub>S<sub>4</sub> to accelerate photocatalytic hydrogen evolution, *Nat. Commun.*, 2022, **13**, 1287.
- 56 T. Liu, W. Gao, Q. Wang, M. Dou, Z. Zhang and F. Wang, Selective Loading of Atomic Platinum on a RuCeO<sub>x</sub> Support Enables Stable Hydrogen Evolution at High Current Densities, *Angew. Chem., Int. Ed.*, 2020, **59**, 20423–20427.
- 57 C. Li, Z. Chen, H. Yi, Y. Cao, L. Du, Y. Hu, F. Kong, R. Kramer Campen, Y. Gao, C. Du, G. Yin, I. Y. Zhang and Y. Tong, Polyvinylpyrrolidone-Coordinated Single-Site Platinum Catalyst Exhibits High Activity for Hydrogen Evolution Reaction, *Angew. Chem., Int. Ed.*, 2020, **59**, 15902–15907.
- 58 J. Zhang, X. Xu, Y. Liu, X. Duan, S. Wang and H. Sun, Platinum single atoms anchored on ultra-thin carbon nitride nanosheets for photoreforming of glucose, *Surf. Interfaces*, 2023, **42**, 103423.
- 59 X. Li, Y. Cao, K. Luo, L. Zhang, Y. Bai, J. Xiong, R. N. Zare and J. Ge, Cooperative catalysis by a single-atom enzyme-metal complex, *Nat. Commun.*, 2022, **13**, 2189.
- 60 Y. Huang, D. Li, S. Feng, Y. Jia, S. Guo, X. Wu, M. Chen and W. Shi, Pt Atoms/Clusters on Ni-phytate-sensitized Carbon Nitride for Enhanced NIR-light-driven Overall Water Splitting beyond 800 nm, *Angew. Chem., Int. Ed.*, 2022, **61**, e202212234.
- 61 S. u Haq, M. S. Khan, E. Djatoubai, C.-L. Dong, P. Guo, Y.-C. Huang and S. Shen, A Facile Approach for Pt Single Atoms Deposition on Two-Dimensional Calcium Niobate Nanosheets for Photocatalytic Hydrogen Evolution, *ACS Sustainable Chem. Eng.*, 2022, **10**, 9096–9104.
- 62 Y. Yu, S. Yang, M. Dou, Z. Zhang and F. Wang, Photochemically activated atomic ruthenium supported on boron-doped carbon as a robust electrocatalyst for hydrogen evolution, *J. Mater. Chem. A*, 2020, **8**, 16669–16675.
- 63 M. Liu, X. Liu, D. Fu, Z. Xie, X. Zou, W. Liu, Y. Yu, J. Wang, H. Wang, C. Tong, Z. Cheng, S. Wu, K. Ding and Y. Yu, A facile complexing agent-assisted single atom Ag-N<sub>3</sub>S<sub>1</sub> site photodeposition strategy, *Appl. Catal., B*, 2022, **318**, 121896.
- 64 A. Majumdar, P. Dutta, A. Sikdar, H. Lee, D. Ghosh, S. N. Jha, S. Tripathi, Y. Oh and U. N. Maiti, Impact of Atomic Rearrangement and Single Atom Stabilization on MoSe<sub>2</sub>@NiCo<sub>2</sub>Se<sub>4</sub> Heterostructure Catalyst for Efficient Overall Water Splitting, *Small*, 2022, **18**, 2200622.



- 65 Q. Chen, Y. Ren, H. Jin, Z. Wang, T. Cheng, T. Sun, J. Tian and Y. Zhu, Icosahedral Pd Nanocrystal Catalysts with Dispersed Bi Atoms via Photochemical Route for Enhanced Formic Acid Oxidation Reaction, *ChemNanoMat*, 2023, **9**, e202300127.
- 66 H. Zhang, Y. Dong, S. Zhao, G. Wang, P. Jiang, J. Zhong and Y. Zhu, Photochemical preparation of atomically dispersed nickel on cadmium sulfide for superior photocatalytic hydrogen evolution, *Appl. Catal., B*, 2020, **261**, 118233.
- 67 W. Fu, J. Wan, H. Zhang, J. Li, W. Chen, Y. Li, Z. Guo and Y. Wang, Photoinduced loading of electron-rich Cu single atoms by moderate coordination for hydrogen evolution, *Nat. Commun.*, 2022, **13**, 5496.
- 68 P. Sharma, M. Sharma, M. Dearg, M. Wilding, T. J. A. Slater and C. R. A. Catlow, Cd/Pt Precursor Solution for Solar H<sub>2</sub> Production and in situ Photochemical Synthesis of Pt Single-atom Decorated CdS Nanoparticles, *Angew. Chem., Int. Ed.*, 2023, **62**, e202301239.
- 69 Y. Zhang, J. Zhou, F. Wang, M. Lv and K. Li, Metal-metal oxide synergistic catalysis: Pt nanoparticles anchored on mono-layer dispersed ZrO<sub>2</sub> in SBA-15 for high efficiency selective hydrogenation, *J. Catal.*, 2023, **421**, 12–19.
- 70 T. Li, J. Liu, Y. Song and F. Wang, Photochemical Solid-Phase Synthesis of Platinum Single Atoms on Nitrogen-Doped Carbon with High Loading as Bifunctional Catalysts for Hydrogen Evolution and Oxygen Reduction Reactions, *ACS Catal.*, 2018, **8**, 8450–8458.
- 71 H. Wei, K. Huang, D. Wang, R. Zhang, B. Ge, J. Ma, B. Wen, S. Zhang, Q. Li, M. Lei, C. Zhang, J. Irawan, L.-M. Liu and H. Wu, Iced photochemical reduction to synthesize atomically dispersed metals by suppressing nanocrystal growth, *Nat. Commun.*, 2017, **8**, 1490.
- 72 P. Zhou, F. Lv, N. Li, Y. Zhang, Z. Mu, Y. Tang, J. Lai, Y. Chao, M. Luo, F. Lin, J. Zhou, D. Su and S. Guo, Strengthening reactive metal-support interaction to stabilize high-density Pt single atoms on electron-deficient g-C<sub>3</sub>N<sub>4</sub> for boosting photocatalytic H<sub>2</sub> production, *Nano Energy*, 2019, **56**, 127–137.
- 73 P. Zhou, X. Hou, Y. Chao, W. Yang, W. Zhang, Z. Mu, J. Lai, F. Lv, K. Yang, Y. Liu, J. Li, J. Ma, J. Luo and S. Guo, Synergetic interaction between neighboring platinum and ruthenium monomers boosts CO oxidation, *Chem. Sci.*, 2019, **10**, 5898–5905.
- 74 R. Xu, B. Xu, X. You, D. Shao, G. Gao, F. Li, X.-L. Wang and Y.-F. Yao, Preparation of single-atom palladium catalysts with high photocatalytic hydrogen production performance by means of photochemical reactions conducted with frozen precursor solutions, *J. Mater. Chem. A*, 2023, **11**, 11202–11209.
- 75 Z. Sun, Y. Yang, C. Fang, Y. Yao, F. Qin, H. Gu, Q. Liu, W. Xu, H. Tang, Z. Jiang, B. Ge, W. Chen and Z. Chen, Atomic-Level Pt Electrocatalyst Synthesized via Iced Photochemical Method for Hydrogen Evolution Reaction with High Efficiency, *Small*, 2022, **18**, 2203422.
- 76 X. Zheng, J. Tang, A. Gallo, J. A. Garrido Torres, X. Yu, C. J. Athanitis, E. M. Been, P. Ercius, H. Mao, S. C. Fakra, C. Song, R. C. Davis, J. A. Reimer, J. Vinson, M. Bajdich and Y. Cui, Origin of enhanced water oxidation activity in an iridium single atom anchored on NiFe oxyhydroxide catalyst, *Proc. Natl. Acad. Sci. U. S. A.*, 2021, **118**, e2101817118.
- 77 Y. Feng, Z. Wang, M. Hua, Y. Liu, L. Jing, L. Wei, Z. Hou, X. Wang, X. Yu, L. Wu, Y. Jiang, J. Deng and H. Dai, Differences between atomically-dispersed and particulate Pt supported catalysts on synergistic photothermocatalytic oxidation of VOCs from cooking oil fumes, *Appl. Catal., B*, 2023, **339**, 123116.
- 78 X. Ge, P. Zhou, Q. Zhang, Z. Xia, S. Chen, P. Gao, Z. Zhang, L. Gu and S. Guo, Palladium Single Atoms on TiO<sub>2</sub> as a Photocatalytic Sensing Platform for Analyzing the Organophosphorus Pesticide Chlorpyrifos, *Angew. Chem., Int. Ed.*, 2019, **59**, 232–236.
- 79 Y. Huang, C. Wang, Y. Yu, Y. Yu, W. Wang and B. Zhang, Atomically Dispersed Ru-Decorated TiO<sub>2</sub> Nanosheets for Thermally Assisted Solar-Driven Nitrogen Oxidation into Nitric Oxide, *CCS Chem.*, 2021, **4**, 1208–1216.
- 80 H. Wei, H. Wu, K. Huang, B. Ge, J. Ma, J. Lang, D. Zu, M. Lei, Y. Yao, W. Guo and H. Wu, Ultralow-temperature photochemical synthesis of atomically dispersed Pt catalysts for the hydrogen evolution reaction, *Chem. Sci.*, 2019, **10**, 2830–2836.
- 81 D. Li, Y. Li, X. Wang, G. Sun, J. Cao and Y. Wang, Surface modification of In<sub>2</sub>O<sub>3</sub> porous nanospheres with Au single atoms for ultrafast and highly sensitive detection of CO, *Appl. Surf. Sci.*, 2023, **613**, 155987.
- 82 J. Zhou, F. Duo, C. Jia, Y. Zhou, C. Wang and Z. Wei, Photochemical Solid-Phase In Situ Anchoring of Single Atoms Ag/g-C<sub>3</sub>N<sub>4</sub> for Enhanced Photocatalytic Activity, *Environ. Eng. Sci.*, 2021, **38**, 1098–1107.
- 83 Z. Shi, X. Zhang, X. Lin, G. Liu, C. Ling, S. Xi, B. Chen, Y. Ge, C. Tan, Z. Lai, Z. Huang, X. Ruan, L. Zhai, L. Li, Z. Li, X. Wang, G.-H. Nam, J. Liu, Q. He, Z. Guan, J. Wang, C.-S. Lee, A. R. J. Kucernak and H. Zhang, Phase-dependent growth of Pt on MoS<sub>2</sub> for highly efficient H<sub>2</sub> evolution, *Nature*, 2023, **621**, 300–305.
- 84 Y. Zhang, L. Guo, L. Tao, Y. Lu and S. Wang, Defect-Based Single-Atom Electrocatalysts, *Small Methods*, 2019, **3**, 1800406.
- 85 P. Liu, R. Qin, G. Fu and N. Zheng, Surface Coordination Chemistry of Metal Nanomaterials, *J. Am. Chem. Soc.*, 2017, **139**, 2122–2131.
- 86 T. Zhang and S. Lu, Sacrificial agents for photocatalytic hydrogen production: Effects, cost, and development, *Chem Catal.*, 2022, **2**, 1502–1505.
- 87 K. Wenderich, K. Han and G. Mul, The Effect of Methanol on the Photodeposition of Pt Nanoparticles on Tungsten Oxide, *Part. Part. Syst. Char.*, 2018, **35**, 1700250.
- 88 W. Jones, D. J. Martin, A. Caravaca, A. M. Beale, M. Bowker, T. Maschmeyer, G. Hartley and A. Masters, A comparison of photocatalytic reforming reactions of methanol and triethanolamine with Pd supported on titania and graphitic carbon nitride, *Appl. Catal., B*, 2019, **240**, 373–379.
- 89 J. Wang, A. S. Cherevan, C. Hannecart, S. Naghdi, S. P. Nandan, T. Gupta and D. Eder, Ti-based MOFs: New insights on the impact of ligand composition and hole



- scavengers on stability, charge separation and photocatalytic hydrogen evolution, *Appl. Catal., B*, 2021, **283**, 119626.
- 90 C. Gomes Silva, R. Juárez, T. Marino, R. Molinari and H. García, Influence of Excitation Wavelength (UV or Visible Light) on the Photocatalytic Activity of Titania Containing Gold Nanoparticles for the Generation of Hydrogen or Oxygen from Water, *J. Am. Chem. Soc.*, 2011, **133**, 595–602.
- 91 J.-J. Li, M. Zhang, B. Weng, J. Chen and H. Jia, Zero-degree photochemical synthesis of highly dispersed Pt/TiO<sub>2</sub> for enhanced photocatalytic hydrogen generation, *J. Alloys Compd.*, 2020, **849**, 156634.
- 92 C. Gao, J. Low, R. Long, T. Kong, J. Zhu and Y. Xiong, Heterogeneous Single-Atom Photocatalysts: Fundamentals and Applications, *Chem. Rev.*, 2020, **120**, 12175–12216.
- 93 Y. Wang, H. Su, Y. He, L. Li, S. Zhu, H. Shen, P. Xie, X. Fu, G. Zhou, C. Feng, D. Zhao, F. Xiao, X. Zhu, Y. Zeng, M. Shao, S. Chen, G. Wu, J. Zeng and C. Wang, Advanced Electrocatalysts with Single-Metal-Atom Active Sites, *Chem. Rev.*, 2020, **120**, 12217–12314.
- 94 R. Qin, Z. Chen, Q. Wu, N. Zheng and P. Liu, Supported atomically dispersed Pd catalyzed direct alkoxylation and allylic alkylation, *Chin. J. Chem.*, 2023, DOI: [10.1002/cjoc.202300516](https://doi.org/10.1002/cjoc.202300516).
- 95 J. Schneider, M. Matsuoka, M. Takeuchi, J. Zhang, Y. Horiuchi, M. Anpo and D. W. Bahnemann, Understanding TiO<sub>2</sub> Photocatalysis: Mechanisms and Materials, *Chem. Rev.*, 2014, **114**, 9919–9986.
- 96 Y. Nosaka and A. Nosaka, Understanding Hydroxyl Radical (<sup>•</sup>OH) Generation Processes in Photocatalysis, *ACS Energy Lett.*, 2016, **1**, 356–359.
- 97 P. Liu, X. Huang, D. Mance and C. Copéret, Atomically dispersed iridium on MgO(111) nanosheets catalyses benzene–ethylene coupling towards styrene, *Nat. Catal.*, 2021, **4**, 968–975.

